NASA TECHNICAL MEMORANDUM

NASA TM-78920

NASA TM-78920

A VISCOUS-INVISCID INTERACTIVE COMPRESSOR CALCULATIONS

by William A. Johnston
Case Western Reserve University
Cleveland, Ohio

and

Peter M. Sockol
Lewis Research Center
Cleveland, Ohio 44135

TECHNICAL PAPER to be presented at the
Eleventh Fluid and Plasma Dynamics Conference
sponsored by the American Institute of Aeronautics and Astronautics
Seattle, Washington, July 10-12, 1978

A VISCOUS-INVISCID INTERACTIVE COMPRESSOR CALCULATION*

William A. Johnston+
Case Western Reserve University
Cleveland, Ohio

Peter M. Sockol++
NASA-Lewis Research Center
Cleveland, Ohio

Abstract

A viscous-inviscid interactive procedure for subsonic flow is developed and applied to an axial compressor stage. Calculations are carried out on a two-dimensional blade-to-blade region of constant radius assumed to occupy a mid-span location. Hub and tip effects are neglected. The Euler Equations are solved by MacCormack's method, a viscous marching procedure is used in the boundary layers and wake, and an iterative interaction scheme is constructed that matches them in a way that incorporates information related to momentum and enthalpy thicknesses as well the displacement thickness. The calculations are quasi-three-dimensional in the sense that the boundary layer and wake solutions allow for the presence of spanwise (radial) velocities.

Nomenclature

B(x)	Lower boundary of the cascade solution region (Fig. 1)
c	Speed of sound
C	Blade chord length
c_p, c_v	Specific heats
e	Total energy (Eq. 4)
f_c	Composite solution vector defined by Eq. 27
$f_b(0)$	Boundary layer solution vector (Fig. 4)
f,g	Vectors defined in Eq. 23
$\vec{\mathcal{F}}, \vec{\mathcal{G}}$	Vectors defined in Eq. 22
F,G,H	Vectors defined by Eq. 4
$(g_b(0))_o$	Vector obtained by evaluating g_o using values obtained from the boundary layer solution, $f_b(0)$, (Eq. 27)
G1,G2,G3, G4	Components of vector G
$\mathcal{G}1, \mathcal{G}2, \mathcal{G}3, \mathcal{G}4$	Components of vector $\vec{\mathcal{G}}$
h	Enthalpy
i,j	Grid indices (Fig. 2)
k	Thermal conductivity
p	Pressure
r,φ,Z	Cylindrical coordinates used in the viscous solution (Fig. 3)
R	Gas constant (Eq. 4)
t	Time
T	Temperature
$\vec{U}$	Vector defined by Eq. 4
u_s, u_n	Velocity components used in the inviscid solution (Fig. 1)
u_x, u_y	Velocity components in the x and y directions (Eqs. 2,3)
u_χ, u_η	Velocity components in the χ and η directions
u,v,w	Velocity components in the ξ,ζ, and η directions (Fig 3)
x,y	Cartesian coordinates used in the inviscid solution (Fig. 1)
χ, γ	Cartesian coordinates used in Section 4 (Fig. 4)
X,Y,Z	Cartesian coordinates used in the viscous solution (Fig. 3)
α,β	Cascade coordinates (Fig. 1)
δ	Boundary layer thickness (Section 4)
δ_N	Boundary layer thickness, nondimensionalized with respect to C(Section 3)
δ^*	Displacement thickness
ε	Small parameter that is $\theta(\frac{C}{\eta})$
θ	angle between B(x) and the x-direction in the cascade solution region (Fig. 1)
μ,λ	Viscosities
ξ,ζ,η	Curvilinear coordinates used in the viscous solution (Fig. 3, Eqs. 11, 12,13)
ρ	Density
ψ	Angle between the ξ-coordinate line and a cylindrical generator (Fig. 3)
Ω	Angular velocity of the blades (rad/sec)

Subscripts

REF	Denotes reference quantity
WALL	Denotes evaluation at wall
o	Denotes evaluation at y=0
δ	Denotes evaluation at y=δ
∞	Denotes evaluation at infinity (Section 3)

Superscripts

′	Denotes derivative (Eqs. 8,9)

I. Introduction

The flow in the blade passages of an axial compressor is quite complicated. In general, the flow is compressible, viscous, unsteady with respect to the blades, turbulent, and highly three dimensional. Furthermore, the flow may be either entirely subsonic or at least partially supersonic. Boundary layer separation may occur at several locations in a compressor blade passage. In addition, any computational attempt to deal realistically with such a flow will encounter these difficulties in a region which is geometrically complex.

For these reasons, it is unlikely that a completely realistic solution of the flow through an

*Work supported by NASA-Lewis Research Center under grant (Graduate Research Program in Aeronautics).
+Now Assistant Professor, School of Engineering Science and Mechanics, Georgia Institute of Technology.
++Research Engineer

entire axial compressor blade passage could be undertaken in the near future. However, a great deal has already been accomplished by examining problems of a simplified nature. The numerical compressor calculations which have been undertaken have tended to examine certain aspects of the flow in a blade passage while ignoring other effects, even though the effects which are omitted from the calculation may be quite important in practice. In this manner, it has been possible to reduce the original problem to one which is mathematically tractable, and to gain some insight into the nature of such a flow.

There have been several approaches to simplification. One approach, presented in detail by Wu[1], consists of the specification of a stream surface within the blade passage and the subsequent solution of the Euler equations on that stream surface. The surface can be specified either as an annular surface (blade to blade) or a meridional surface (hub to shroud), and by confining the calculation to a two-dimensional region in this fashion, it is possible to introduce the passage geometry into the calculation while retaining the numerical benefits of a scalar stream function. This technique has been used by Katsanis[2] and Katsanis and McNally[3], among others. The computer codes of references 2 and 3 are well established, and are currently used in compressor design.

Boundary layer calculations have been done on compressor blades and on passage endwalls[4-6]. Similar to boundary layer calculations are the viscous marching procedures, which are used to solve parabolized Navier-Stokes equations[7-8]. Viscous marching procedures are currently being applied to flow in turbomachinery.

Another popular simplification of compressor flow is its idealization as flow through a cascade of airfoils. Many different numerical solutions have been carried out in cascade geometries. Perhaps the most studied set of equations with reference to cascade geometries are the Euler equations, and a popular approach to their numerical solution has been through time marching techniques[10-12]. These techniques, of which MacCormack's method[13] has been the most widely used, owe their popularity to several factors. They are computationally efficient, they can be used for both subsonic and supersonic flow, and they are not subject to some of the limitations of simpler solution methods, such as irrotationality and two-dimensionality. And certain recently developed time marching algorithms[14-16], which are applicable to the solution of the Euler equations and Navier-Stokes equations, appear to be quite promising for increased computational efficiency. It is likely that these new algorithms, or variants of them, will be used in the near future to carry out compressor calculations of increasing sophistication.

While the preceding survey of numerical compressor calculations is by no means complete, it serves to demonstrate the diversity of approaches to the overall problem, which is too difficult to be attacked in a more straightforward manner. The present investigation is primarily concerned with the effect of viscosity on the flow in a blade-to-blade surface of constant radius, which may be assumed to occupy a mid-span location since the effects of the hub and tip regions are neglected. The investigation has been confined to subsonic flows, but this limitation is not inherent in the method developed here. For the present discussion the solution surface can be considered to be the flat, two-dimensional region of a rectilinear cascade, with cambered blades of zero thickness. However it will eventually be necessary to imagine this flat solution region as being wrapped onto the surface of a rotating right circular cylinder. The introduction of viscosity into the calculation is accomplished by means of a viscous-inviscid interactive calculation procedure.

The inviscid calculation consists of a time-marching solution of the Euler equations by MacCormack's Method. The viscous calculation proceeds in boundary layer and wake regions, and it solves a system of equations analogous to the set obtained by Horlock and Wordsworth[4] for the incompressible boundary layer on a helical blade. Although the viscous calculation is carried out on a cylindrical surface, the governing system of equations allows for the presence of a radial velocity component normal to that surface. The interaction between the viscous and inviscid calculations is accomplished by means of an iterative process. An iterative approach to the subsonic interaction problem is not uncommon; several researchers (e.g., Ref. 17-18) have used this approach, in conjunction with the displacement thickness concept[19] to obtain higher approximations to flows. However, the present interactive method differs from these procedures in two ways. First, the present method does not rely solely on the mechanism of a physical displacement of the outer flow streamlines by the viscous layer, to achieve coupling of the viscous and inviscid calculations. The interaction takes the form of an injection at blade surfaces (suction in the wake), but it is different from the usual source-sink distribution technique in that this injection has a momentum and enthalpy character. Second, the application of boundary conditions to the viscous calculation, and the viscous calculation itself are carried out in a manner suggested by the theory of matched asymptotic expansions. The details of the interactive procedure are discussed in Section IV.

The viscous-inviscid interactive calculation procedure which is described in this paper was used to calculate compressor flows for both rotor and stator passages. Some results of these numerical calculations are presented.

II. The Inviscid Solution

For the inviscid solution we consider the inviscid, rotational flow in a rectilinear cascade of zero thickness airfoils. The (α,β) coordinate system used for this calculation (Fig. 1) is related to Cartesian coordinates by the relations,

$$\alpha = x \quad , \quad \beta = y - B(x) \tag{1}$$

Also seen in Fig. 1 are the velocity components u_s and u_n, which are related to the Cartesian components of velocity in the following manner;

$$u_x = u_s \cos\theta - u_n \sin\theta \tag{2}$$

$$u_y = u_s \sin\theta + u_n \cos\theta \tag{3}$$

For this coordinate system the time dependent Euler equations may be written in vector form as,

$$\frac{\partial U}{\partial t} + \frac{\partial F}{\partial \alpha} + \frac{\partial G}{\partial \beta} + H = 0 \qquad (4)$$

where,

$$U = \begin{bmatrix} \rho \\ \rho u_s \\ \rho u_n \\ e \end{bmatrix}, \quad F = \begin{bmatrix} \rho u_x \\ \rho u_x u_s + p \cos\theta \\ \rho u_x u_n - p \sin\theta \\ (e + p)\, u_x \end{bmatrix},$$

$$G = \begin{bmatrix} \rho u_n \sec\theta \\ \rho u_s u_n \sec\theta \\ (\rho u_n^2 + p) \sec\theta \\ (e + p)\, u_n \sec\theta \end{bmatrix}, \quad H = \begin{bmatrix} 0 \\ -(\rho u_x u_n - p \sin\theta)\frac{d\theta}{d\alpha} \\ (\rho u_x u_s + p \cos\theta)\frac{d\theta}{d\alpha} \\ 0 \end{bmatrix}$$

with $e = \rho[c_v T + \frac{1}{2}(u_x^2 + u_y^2)]$ and $p = \rho RT$.

A steady state solution of these equations in the cascade is obtained by a numerical time marching solution using MacCormack's Method[13].

Boundary Conditions

As is often the case with time marching solutions of the Euler equations, the treatment of boundary conditions here consumes a disproportionately large part of the effort expended in the numerical solution. A careful treatment of certain boundary conditions in such problems seems to demand approaches which are somewhat involved. The discussion of boundary conditions which appears in this section deals entirely with conditions as they exist for the first inviscid solution. Modifications to these boundary conditions are required for subsequent inviscid solutions within the viscous-inviscid iteration scheme, and a discussion of these modifications is deferred until Section IV.

In a time marching solution of the Euler Equations for the flow through a cascade (Fig. 1), essentially three different types of boundary regions are encountered. First, boundaries at which periodicity conditions are the proper specification. This is the case at those portions of the boundary which connect the leading and trailing edges of the blades to the upstream and downstream boundaries. Second, the upstream and downstream boundaries which in this investigation are subsonic and permeable. It appears necessary that the specification of boundary conditions at these locations be compatible with the passage of wavelike disturbances through the boundary[20]. Consequently, we treat the boundary conditions at these locations using the method of characteristics as suggested by Moretti[21]. The details of this treatment are found in Reference 22. Finally, solid wall boundaries represent a third type of situation. As the treatment of solid wall boundary conditions is altered in subsequent inviscid solutions within the interactive scheme, we describe the situation during the first inviscid solution in some detail, so that the changes made for later solutions will be more apparent.

Consider the numerical grid network near a blade surface which is depicted in Fig. 2. The grid lines j=2 and j=3 lie in the interior of the solution region, and solution values at these locations are obtained from the MacCormack algorithm. The j=1 grid line is a dummy point location, and it is at this location that the boundary conditions are applied. The impermeability of the wall gives three relations, since three components of the vector G (see Eq. (4)) are identically zero. The effected components are G1, G2, and G4, where the numbers correspond to the position of the component within the vector. These relations are,

$$G1_{i,1} = -G1_{i,2} \qquad (5)$$

$$G2_{i,1} = -G2_{i,2} \qquad (6)$$

$$G4_{i,1} = -G4_{i,2} \qquad (7)$$

The remaining component, G3, reduces to (p sec θ). A fourth relation is obtained by again appealing to the method of characteristics. Following Moretti[21], we seek to resolve those waves which propagate in a direction normal to the boundary, apart from a translation tangent to the boundary due to the gross motion of the fluid. Using this approach we obtain (see Ref. 22) the compatibility relation,

$$p' - \rho c u_n' = -\rho c\Big(c\frac{\partial}{\partial\alpha}(u_s \cos\theta) - c u_n \cos\theta \frac{d\theta}{d\alpha} - u_s u_x \frac{d\theta}{d\alpha}\Big) \qquad (8)$$

where c is the speed of sound, and the primes denote differentiation in a direction defined by,

$$\frac{d\alpha}{dt} = u_x + c\sin\theta, \quad \frac{d\beta}{dt} = \sec\theta(u_n - c) \qquad (9)$$

Equation (8) may be integrated along a bicharacteristic line defined by Eq. (9) to obtain the wall pressure. Having obtained the wall pressure in this manner, a fourth relation is then available of the form,

$$G3_{i,1} = 2(p_{WALL})_i(\sec\theta)_i - G3_{i,2} \qquad (10)$$

As a final note in this section, we mention that the Kutta condition is applied at the trailing edge of the blades by enforcing flow tangency.

Extension to the Annular Cascade

As a preliminary to the discussion of the viscous solution, it is worth noting that the numerical solution for the inviscid flow in a rectilinear cascade can be related to the flow in an annular cascade in a fairly simple way. To extend the results of the previous solution to the flow on a surface of constant radius which is in a state of radial equilibrium (i.e., zero radial velocity) and rotates about its axis, it is merely necessary to imagine that the flat solution field is wrapped onto the surface of a rotating right circular cylinder.

III. The Viscous Solution

In this section, we develop the viscous equations appropriate to the flow past cambered, yet strictly radial, blades. These blades and the coordinate system used in this development are seen in Fig. 3. The (ξ,ζ,η) coordinate system used in this section is shown in relation to a Cartesian coordinate system (X,Y, Z), and a cylindrical coordinate system (r,ϕ,Z). The ξ and ζ coordinate lines are shown on a cylindrical surface (η=r= const.). The angle $\psi(\xi)$, which is measured on that surface, is the angle between the ξ coordinate line

and a generator of the surface. If we describe the ξ coordinate line as a helix-like curve of angle ψ, then the ζ coordinate line will be a helix-like curve of angle $(270^o + \psi)$. The η coordinate lines are straight lines normal to the surface of the cylinder. Finally, the velocity components in the ξ, ζ and η directions are denoted by u, v and w, respectively.

The curvilinear coordinates are related to Cartesian coordinates in the following way;

$$Z = \int_o^{\xi} \cos\psi \, d\xi + \zeta \sin\psi \tag{11}$$

$$X = \eta \cos\varphi \; ; \quad Y = \eta \sin\varphi \tag{12,13}$$

where,

$$\varphi = \frac{\int_o^{\xi} \sin\psi d\xi - \zeta \cos\psi}{\eta}$$

Following Horlock and Wordsworth[4], we confine our attention to the blade boundary layers which develop in a system that rotates about the Z axis with an angular velocity Ω, and make some specification and assumptions.

(i) Radial equilibrium is specified for the external flow ($w_\infty = 0$). The ∞ subscript indicates a location where ζ is large.

(ii) The boundary layer thickness is small compared to the blade chord;

$$\frac{\zeta}{C} \sim \theta(\delta_N) \quad \text{where } \delta_N \ll 1.$$

(iii) The chordwise curvature of the blade is of order $(\frac{1}{C})$. This implies that

$$C \frac{\partial\psi}{\partial\xi} \sim \mathcal{O}(1),$$

and that $\zeta \frac{\partial\psi}{\partial\xi} \sim \mathcal{O}(\delta_N)$.

(iv) The chord is small compared to the radius,

$$\frac{\eta}{C} \sim (\frac{1}{\epsilon}) \text{ where } \epsilon \ll 1 .$$

(v) The blade speed and u_∞ are of like order;

$$\frac{\Omega\eta}{u_\infty} \sim \mathcal{O}(1) .$$

For a turbomachine it is expected that $\delta_N \ll \epsilon$.

With the ordering procedure established here, it is possible to reduce the equations of motion for the helical coordinate system to the appropriate boundary layer equations. The details of this reduction may be found in Ref. 22. The boundary layer equations, correct to $\mathcal{O}(\epsilon)$, which result are as follows:

$$\frac{\partial}{\partial\xi}(\rho u) + \frac{\partial}{\partial\zeta}(\rho v) = 0 \tag{14}$$

$$\rho u \frac{\partial u}{\partial\xi} + \rho v \frac{\partial u}{\partial\zeta} = \rho_\infty u_\infty \frac{\partial u_\infty}{\partial\xi} + \frac{\partial}{\partial\zeta}(\mu \frac{\partial u}{\partial\zeta}) \tag{15}$$

$$\rho u \frac{\partial w}{\partial\xi} + \rho v \frac{\partial w}{\partial\zeta} = \frac{(\rho u^2 - \rho_\infty u_\infty^2)\sin^2\psi}{\eta} \tag{16}$$

$$+ \eta\Omega^2(\rho - \rho_\infty) + 2\Omega \sin\psi \, (\rho v - \rho_\infty u_\infty) + \frac{\partial}{\partial\zeta}(\mu \frac{\partial w}{\partial\zeta})$$

$$\rho u \frac{\partial h}{\partial\xi} + \rho v \frac{\partial h}{\partial\zeta} = u(\rho_\infty \frac{\partial h_\infty}{\partial\xi}) + \mu(\frac{\partial u}{\partial\zeta})^2 + \frac{\partial}{\partial\zeta}(k \frac{\partial T}{\partial\zeta}) \tag{17}$$

The radial momentum equation (16) is uncoupled from the other three equations in the sense that the radial velocity (w) and the radial coordinate (η) do not appear in Eqs. (14,15,or 17). Consequently, if we confine our attention to a surface of constant radius (η=const.), it is possible to solve this system of equations with the appropriate boundary conditions by numerical marching techniques[23]. To complete this system of equations, we take as the equation of state,

$$p = \rho RT \tag{18}$$

and take the enthalpy, viscosity, and thermal conductivity to be governed by the relations;

$$h = c_p T \tag{19}$$

$$\mu = \mu_{REF}(T/T_{REF})^{.76} \tag{20}$$

$$k = k_{REF}(T/T_{REF})^{.84} \tag{21}$$

Eqs. (14-21) are also the governing equations for the viscous wake.

It should be noted that, while the inviscid and viscous calculations are both carried out on the same cylindrical surface, the coordinate systems used in these two calculations are different and the numerical grid systems would not in general coincide nor have the same orientation.

IV. The Interactive Procedure

The interactive procedure takes the form of an iteration between viscous and inviscid solutions. In general terms, this iterative procedure is as follows:

(i) An inviscid solution for the entire flowfield is performed, with the appropriate boundary conditions.

(ii) Using boundary conditions, obtained from the inviscid solution along blade surfaces and the wake centerline, the viscous calculation is carried out. With the viscous calculation completed, certain adjustments are made in the inviscid solution's boundary conditions, to reflect the presence of viscous layers.

(iii) Steps (i) and (ii) are repeated until an acceptable degree of convergence is obtained.

We now attend to the actual form of this interaction.

The Euler equations for steady flow may be written, in Cartesian coordinates, in the vector form

$$\frac{\partial \vec{f}}{\partial x} + \frac{\partial \vec{h}}{\partial y} = 0 \tag{22}$$

where

$$\vec{f} = \begin{bmatrix} \rho u_x \\ \rho u_x^2 + p \\ \rho u_x u_y \\ u_x(e + p) \end{bmatrix} \qquad \vec{h} = \begin{bmatrix} \rho u_y \\ \rho u_x u_y \\ \rho u_y^2 + p \\ u_y(e + p) \end{bmatrix}$$

Also, the steady Navier-Stokes equations may be written in the vector form

$$\frac{\partial f}{\partial x} + \frac{\partial g}{\partial y} = 0 \qquad (23)$$

where;

$$f = \begin{bmatrix} \rho u_x \\ \rho u_x^2 + p - \lambda\left(\frac{\partial u_x}{\partial x} + \frac{\partial u_y}{\partial y}\right) - 2\mu \frac{\partial u_x}{\partial x} \\ \rho u_x u_y - \mu\left(\frac{\partial u_x}{\partial y} + \frac{\partial u_y}{\partial x}\right) \\ u_x\left(e + p - \lambda\left(\frac{\partial u_x}{\partial x} + \frac{\partial u_y}{\partial y}\right) - 2\mu \frac{\partial u_x}{\partial x}\right) \\ \quad - u_y\mu\left(\frac{\partial u_x}{\partial y} + \frac{\partial u_y}{\partial x}\right) + k \frac{\partial T}{\partial x} \end{bmatrix},$$

$$g = \begin{bmatrix} \rho u_y \\ \rho u_x u_y - \mu\left(\frac{\partial u_x}{\partial y} + \frac{\partial u_y}{\partial x}\right) \\ \rho u_y^2 + p - \lambda\left(\frac{\partial u_x}{\partial x} + \frac{\partial u_y}{\partial y}\right) - 2\mu \frac{\partial u_y}{\partial y} \\ u_y\left(e + p - \lambda\left(\frac{\partial u_x}{\partial x} + \frac{\partial u_y}{\partial y}\right) - 2\mu \frac{\partial u_y}{\partial y}\right) \\ \quad - u_x\mu\left(\frac{\partial u_x}{\partial y} + \frac{\partial u_y}{\partial x}\right) + k \frac{\partial T}{\partial y} \end{bmatrix}$$

Now, we consider the flow in the immediate vicinity of the wall, where the viscosity and thermal conductivity are important. We suppose that this viscous strip is sufficiently thin (compared to the radius of curvature of the wall), and that the chordwise extent of the region under consideration is for the present sufficiently small, so that we are justified in covering this region with a Cartesian coordinate system (see Fig. 4). An exact representation of the flow in this region is given by a solution of the Navier-Stokes equations. Let f and g be the vectors constructed from this solution. Also, we suppose that some solution of the Euler equations will provide a close approximation of the exact solution when $y > \delta$, and let $\mathcal{F}$ and $\mathcal{G}$ be the vectors constructed from this inviscid solution. Having identified the vectors f, g, $\mathcal{F}$, and $\mathcal{G}$ with these two solutions, Eqs. (22) and (23) may be integrated from y=0 to y=δ, to give;

$$\mathcal{G}_\delta - \mathcal{G}_o = -\frac{\partial}{\partial x}\int_o^\delta \mathcal{F}\, dy \qquad (24)$$

$$g_\delta - g_o = -\frac{\partial}{\partial x}\int_o^\delta f\, dy \qquad (25)$$

Since the two solutions are taken to coincide for $y > \delta$, we may specify $\mathcal{G}_\delta = g_\delta$. Eqs. (24) and (25) may be combined then to give,

$$\mathcal{G} = g_o + \frac{\partial}{\partial x}\int_o^\delta (\mathcal{F} - f)\, dy \qquad (26)$$

Eq. (26), which relates the two hypothetical solutions, will serve as a starting point for our discussion of the solution technique in the viscous layer.

It is not our intention to solve the Navier-Stokes equations, therefore, we seek a suitable approximation of f and g on the interval $0 \le y \le \delta$. We represent the exact solution by a composite function, f_c, where

$$f_c = \mathcal{F} + f_b(0) - \mathcal{F}_o \qquad (27)$$

These functions are shown in Fig. 4; $f_b(0)$ corresponds to a boundary layer solution carried out using inviscid values at $y = 0$ as boundary conditions. The composite function f_c is constructed in the spirit of a matched asymptotic expansion. The function f_c was chosen as an approximation of the exact solution for two reasons. First, we expect that this approach will have greater accuracy than the usual boundary layer solution. Second, we employ f_c because it has distinct computational advantages within the context of the iterative procedure.

Applying Eq. (27) to Eq. (26) gives,

$$\mathcal{G}_o = (g_b(0))_o + \frac{\partial}{\partial x}\int_o^\delta (\mathcal{F}_o - f_b(0))\, dy \qquad (28)$$

Eq. (28) can be used as the basis for an iterative solution technique in the following way:

(i) $(\mathcal{G}1)_o$, $(\mathcal{G}2)_o$ and $(\mathcal{G}4)_o$ are initially set equal to zero, and an inviscid solution is carried out.

(ii) Using inviscid values at $y=0$, a boundary layer solution is performed.

(iii) Using values obtained from the inviscid and boundary layer solutions, Eq. (28) is solved for new values of $(\mathcal{G}1)_o$, $(\mathcal{G}2)_o$ and $(\mathcal{G}4)_o$. The vector component $(\mathcal{G}3)_o$ which contains the surface pressure is evaluated using the method of characteristics. Since Eq. (28) requires only surface values from the inviscid solution, a minimum of interpolation is required between the viscous and inviscid grid systems.

The interaction model which has been described here can be conveniently used with those inviscid solution procedures, which are currently employed to solve the Euler equations in primitive variable form. There is an alternative method for dealing with the numerical viscous-inviscid interaction when the inviscid flow is rotational, that being the displacement thickness approach, but it is not conveniently used in a problem involving complicated geometries. In such an approach, bodies are physically thickened, and it would be necessary to recompute the geometry of the problem at each step in the iteration. In the present method, the geometry of the solid surface must be dealt with only once, and remains unchanged throughout the iterative process.

The form which the interaction takes in the blade wake is similar to the case of a wall boundary layer, which has been described. The details of the wake calculation are not reproduced here;

for these the reader is referred to Reference 22.

V. Numerical Results

In this section we present some results obtained by applying this interactive calculation procedure to the flow in a cascade of zero-thickness airfoils, whose shape is that of a NACA, a = .4 mean line, with C_{L_i} = .1 (see Ref. 24). The stagger angle of the cascade is 15°, the chordlength of the blades is .3 ft., and the blade spacing is .2 ft. We consider a subsonic flow of air through this cascade. The calculation takes place on a cylindrical surface of radius 2.5 ft., and we consider both a rotor passage (angular velocity, 200 rad/sec), and a stator passage (zero angular velocity). Due to the nature of the equations which we are solving these two cases will differ only in the radial velocities in the boundary layers and wake which result.

In Figs. 5-8, values of the streamwise velocity (u_s) and density (ρ) are plotted along several β = const. grid lines, where the location of the suction surface corresponds to β = 0 ft., and the location of the pressure surface corresponds to β = .2 ft. The viscous-inviscid iterative scheme was run for four global iterations, and values from the first and last inviscid solutions are seen in these figures. The leading edge is denoted as L.E., and the trailing edge by T.E. A noteworthy feature of these plots may be seen by comparing the first and last inviscid solution values. Once the injection-suction boundary conditions are applied, an effective bluntness is introduced at the leading edge. Also, an effective displacement body surrounds the trailing edge. The new situation is numerically less severe, and it may be seen that a small waviness in the solution, which is apparent upstream and downstream of the blades, now disappears. The final solution values at the leading edge behave as though a stagnation point had developed in the vicinity.

An important advantage of an interactive calculation over a single inviscid calculation with a boundary layer added can be seen by comparing the flow in the immediate vicinity of the trailing edge in Figs. 5 and 6. At this location the interaction between the viscous flow and the inviscid flow is strong, and the shape of the velocity profile changes significantly between the first and last inviscid solutions. In Fig. 6, a rapid deceleration of the fluid is indicated slightly downstream of the trailing edge. A single inviscid solution with a boundary layer added would not resolve this behavior.

In Figs. 9 and 10, we plot rotor and stator radial velocity profiles for pressure surface boundary layer and wake locations. The plots in Figs. 9 and 10 are taken from the final (fourth) viscous solution at locations about one third of a chord length behind the leading and trailing edges respectively. It may be seen that there is a large difference between the profiles obtained for a rotor passage and a stator passage, at both wake and boundary layer locations. For a rotor passage the velocities are radially outward, and for a stator passage the velocities are radially inward. Also, it may be noted that generally larger values of the radial velocity are obtained in the wake than in the blade boundary layers.

As an illustration of the computer program's successful operation, values of the displacement thickness (δ^*) are plotted over a portion of the suction surface, for each of the four viscous solutions (Fig. 11). We have limited the chordwise extent of the region under consideration in order to expand the vertical (δ^*) scale, so that the convergence characteristics of the global iterative scheme would be clearly visible. The abscissa in Fig. 11 corresponds to distance along the blade surface, measured from the leading edge. The behavior of successive solutions in Fig. 11 indicates convergence. Also, it appears that this convergence takes place quite rapidly, since the third and fourth solutions are virtually indistinguishable even at this expanded scale.

VI. Discussion

The numerical results of the preceding section were taken from two solutions (rotor and stator) which were carried out on an inviscid grid with 90 x 20 dimensions. The two calculations, which each required about 22 minutes (C.P.U. time) on a UNIVAC 1110, were run for four global iterations. The inviscid calculation procedure accounted for most of the run time.

The computer program which has been developed in the course of this study is currently limited in its ability to simulate real compressor flows by the idealizations which have been made. Idealizations such as blades of zero-thickness and strictly laminar flow have been introduced to simplify the computational problem, but it is important to note that these idealizations are not inherent in our general approach to the viscous-inviscid interaction. The interactive calculation procedure which is presented here does not rely for its successful operation on the geometrical simplifications which have been made, and even depends very little on the precise form of the viscous and inviscid solutions. For example, an integral boundary layer calculation could be substituted for the present viscous marching procedure, or an implicit time marching algorithm used to solve the inviscid equations, and the overall nature of the interactive calculation would not be much affected. This interactive scheme is novel in that it does not rely solely on the boundary layer displacement thickness, but incorporates information related to momentum and enthalpy thicknesses as well. The form of the interactive calculation procedure conveniently accomodates inviscid solution procedures which are currently used to solve the Euler equations in primitive variable form, and appears to have certain computational advantages for dealing with the viscous-inviscid interaction when the inviscid flow is rotational.

Acknowledgment

The authors wish to express their appreciation to Professor Eli Reshotko of Case Western Reserve University for the technical advice and direction which he provided during the course of this work.

References

1. Wu, C. H., A General Theory of Three Dimensional Flow in Subsonic Turbomachines of Axial, Radial and Mixed Flow Types, NACA TN 2604 (1952).
2. Katsanis, Theodore, FORTRAN Program for Calculating Transonic Velocities on a Blade-to-Blade Stream Surface of a Turbomachine, NASA TN D-5427 (1969).
3. Katsanis, Theodore and McNally, William D., FORTRAN Program for Calculating Velocities and Streamlines on the Hub-Shroud Mid-Channel Flow Surface of an Axial- or Mixed-Flow Turbomachine, Rev.--User's Manual, NASA TN D-7343 (1973).
4. Horlock, J. H. and Wordsworth, J., The Three-Dimensional Laminar Boundary Layer on a Rotating Helical Blade, J. Fluid Mech., Vol. 23, Pt. 2, pp. 305-314 (1965).
5. Miyake, Y. and Fujita, S., A Laminar Boundary Layer on a Rotating Three-Dimensional Blade, J. Fluid Mech., Vol. 65, Pt. 3, pp. 481-498 (1974).
6. Mellor, G. H. and Wood, G. M., An Axial Compressor End Wall Boundary Layer Theory, Trans., ASME J. of Basic Eng., Vol. 93, No. 2 (1971).
7. Caretto, L. S., Curr, R. M. and Spalding, D. B., Two Numerical Methods for Three-Dimensional Boundary Layers, Computer Meth. in Appl. Mech. and Eng., 1, pp. 39-57 (1972).
8. Briley, W. Roger, Numerical Method for Predicting Three-Dimensional Steady Viscous Flow in Ducts, J. Comp. Phys., Vol. 14, No. 1 (1974).
9. Delaney, R. A. and Kavanagh, P., Transonic Flow Analysis in Axial-Flow Turbomachinery Cascades By a Time-Dependent Method of Characteristics, Technical (Final) Report, ERI-74034, Iowa State University, Ames, Iowa, May 1974.
10. Kurzrock, John W. and Novick, Allen S., Transonic Flow Around Compressor Rotor Blade Elements, Vol. 1: Analysis. Air Force Aero Propulsion Laboratory Report, AFAPL-TR-73-69, Vol. 1, Aug. 1973.
11. Gopalkrishnan, S. and Bozzola, R., A Numerical Technique for the Calculation of Transonic Flows in Turbomachinery Cascades, ASME Paper No. 71-GT-42, Gas Turbine Conference and Products Show, Houston, TX, March 1971.
12. Erdos, J., Alzner, E., Kalben, P., McNally, W. and Slutsky, S., Time Dependent Transonic Flow Solutions for Axial Turbomachinery, NASA SP-347, Part I, pp. 587-621 (1975).
13. MacCormack, R. W., Numerical Solution of the Interaction of a Shock Wave with a Laminar Boundary Layer, Lecture Notes in Physics, Vol. 8, Springer-Verlag, New York, pp. 151-163 (1971).
14. Briley, W. R. and McDonald, H., An Implicit Numerical Method for the Multidimensional Compressible Navier-Stokes Equations, United Aircraft Research Laboratories Report M911363-6, Nov. 1973.
15. Beam, R. M. and Warming, R. F., An Implicit Finite Difference Algorithm for Hyperbolic Systems in Conservation Law Form, J. Comp. Phys., Vol. 22, No. 1, pp. 87-110 (1976).
16. MacCormack, R. W., An Efficient Numerical Method for Solving the Time-Dependent Compressible Navier-Stokes Equations at High Reynolds Number. Paper presented at the ASME 97th Winter Annual Meeting, New York, December 5-10, 1976.
17. Olson, L. E. and Dvorak, F. A., Viscous/Potential Flow about Multi-Element Two-Dimensional and Infinite-Span Swept Wings: Theory and Experiment, NASA TM X-62, 513 (1975).
18. Brune, G. W., Rubbert, P. E. and Nark, T. C., A New Approach to Inviscid Flow/Boundary Layer Matching, AIAA Paper No. 74-601 (1974).
19. Lighthill, M. J., On Displacement Thickness, J. Fluid Mech., Vol. 4, Pt. 4, pp. 383-392 (1958).
20. Moretti, G., Importance of Boundary Conditions in the Numerical Treatment of Hyperbolic Equations. High Speed Computing in Fluid Dynamics, Physics of Fluids Supplement II, pp. II-13 — II-20 (1969).
21. Moretti, G., The Choice of a Time-Dependent Technique in Gas Dynamics, PIBAL Report No. 69-26, Polytechnic Institute of Brooklyn, July 1969.
22. Johnston, W. Sockol, P. and Reshotko, E., A Viscous-Inviscid Interactive Compressor Calculation. Report FTAS/TR-78-136, Dept. of Mech. and Aerospace Eng., Case Western Reserve University, March 1978.
23. Hornbeck, R. W., Numerical Marching Techniques for Fluid Flows with Heat Transfer, NASA SP-297 (1973).
24. Abbott, I. H. and Von Doenhoff, A. E., Theory of Wing Sections, Dover (1959).

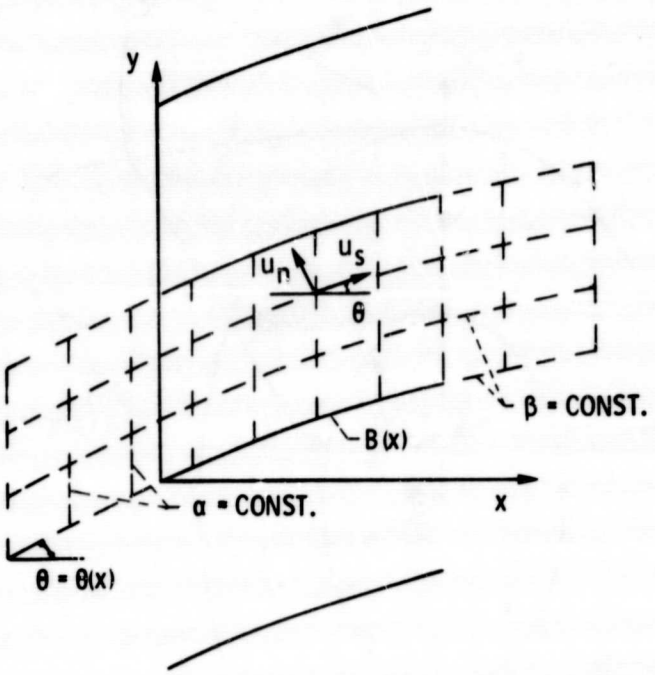

Figure 1. - The cascade coordinate system.

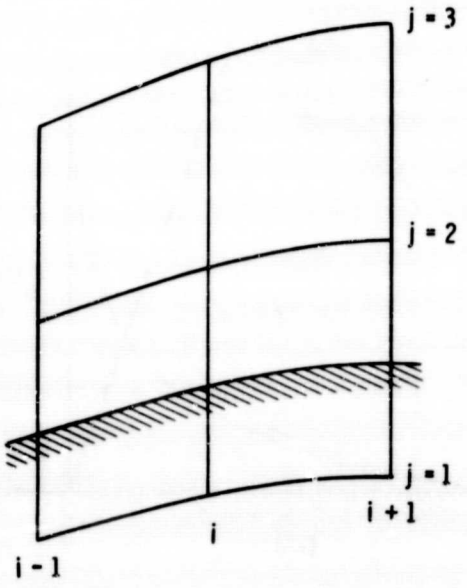

Figure 2. - Grid lines in the neighborhood of a blade surface.

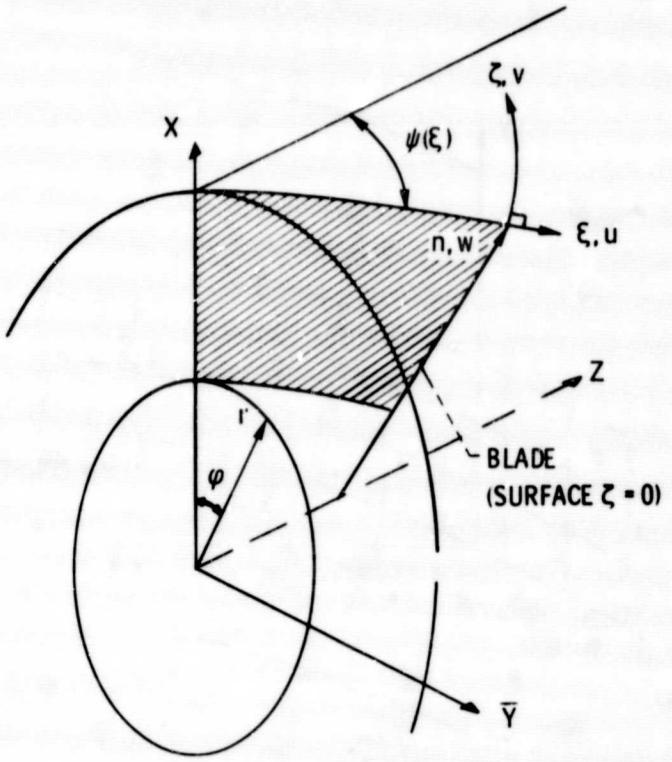

Figure 3. - The coordinate system for the viscous solution.

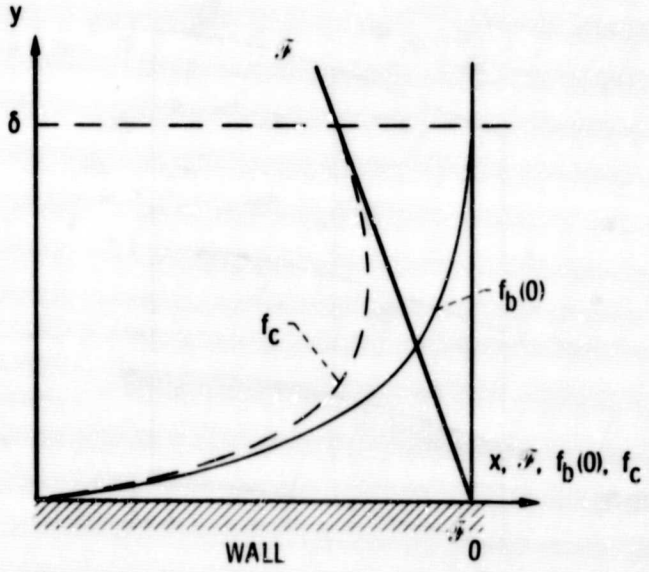

Figure 4. - The inviscid, boundary layer, and composite solutions.

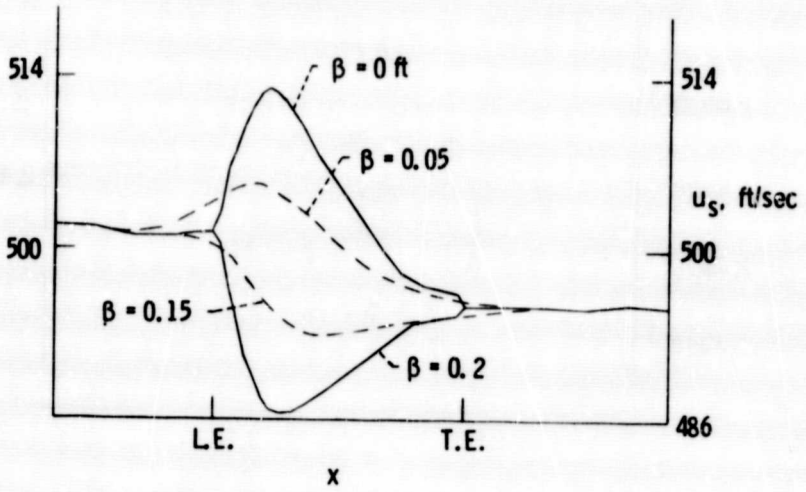

Figure 5. - Chordwise velocity (first inviscid solution).

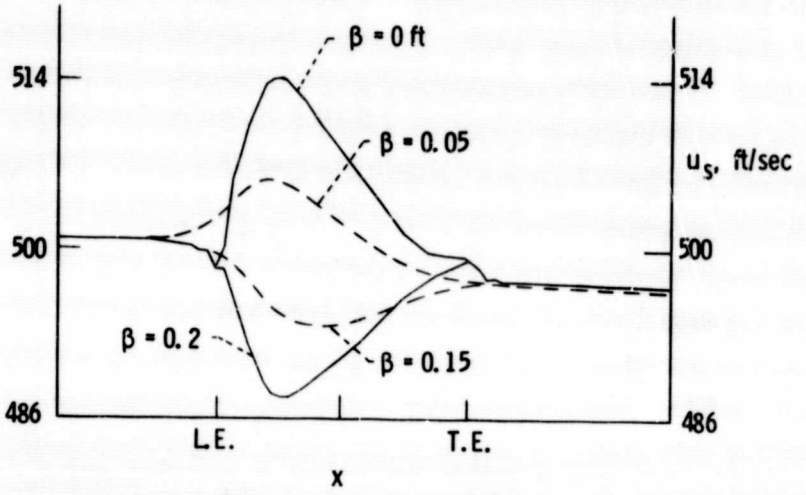

Figure 6. - Chordwise velocity (fourth inviscid solution).

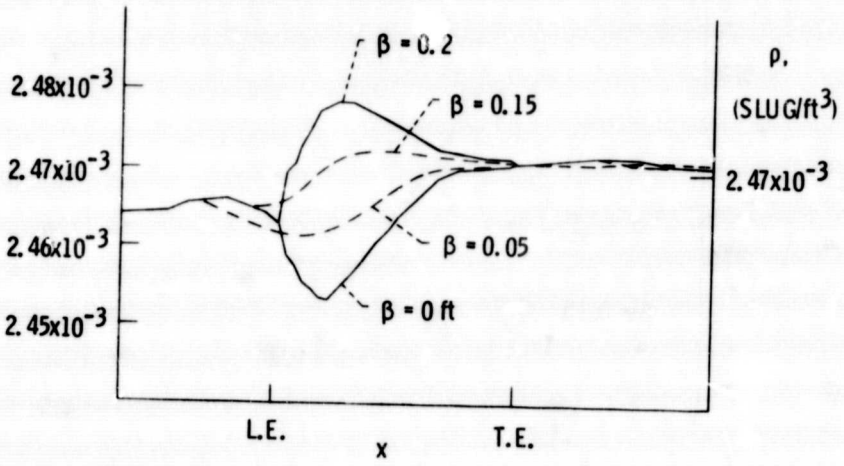

Figure 7. - Density (first inviscid solution).

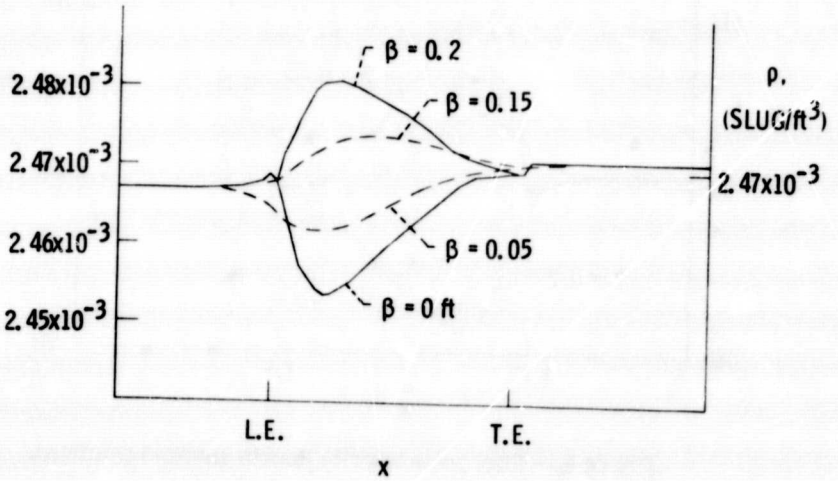

Figure 8. - Density (fourth inviscid solution).

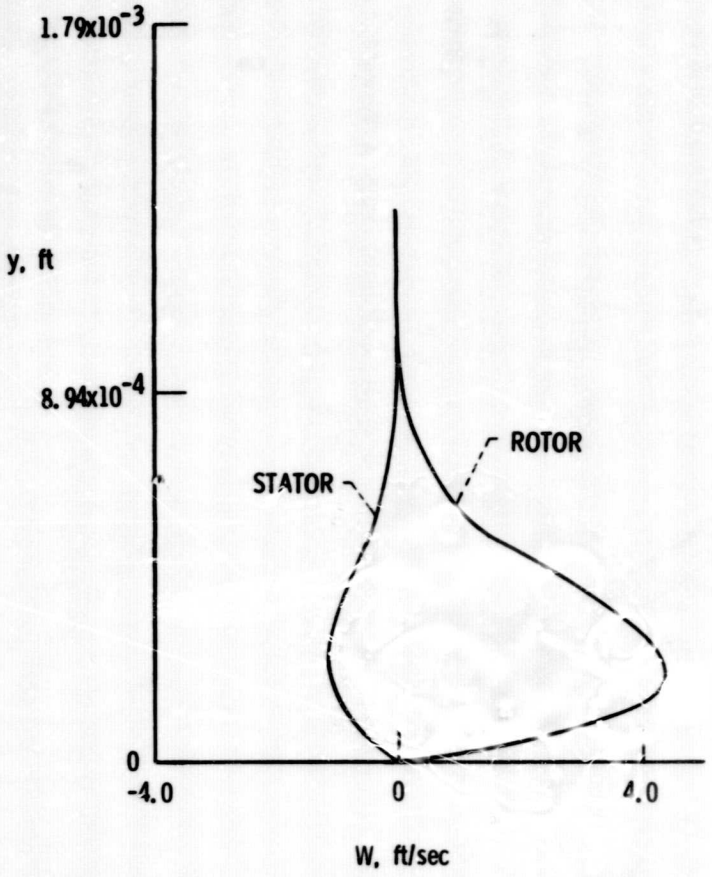

Figure 9. - Radial velocity, pressure surface, for rotor (Ω = 200 rad/sec) and stator (Ω = 0) cases.

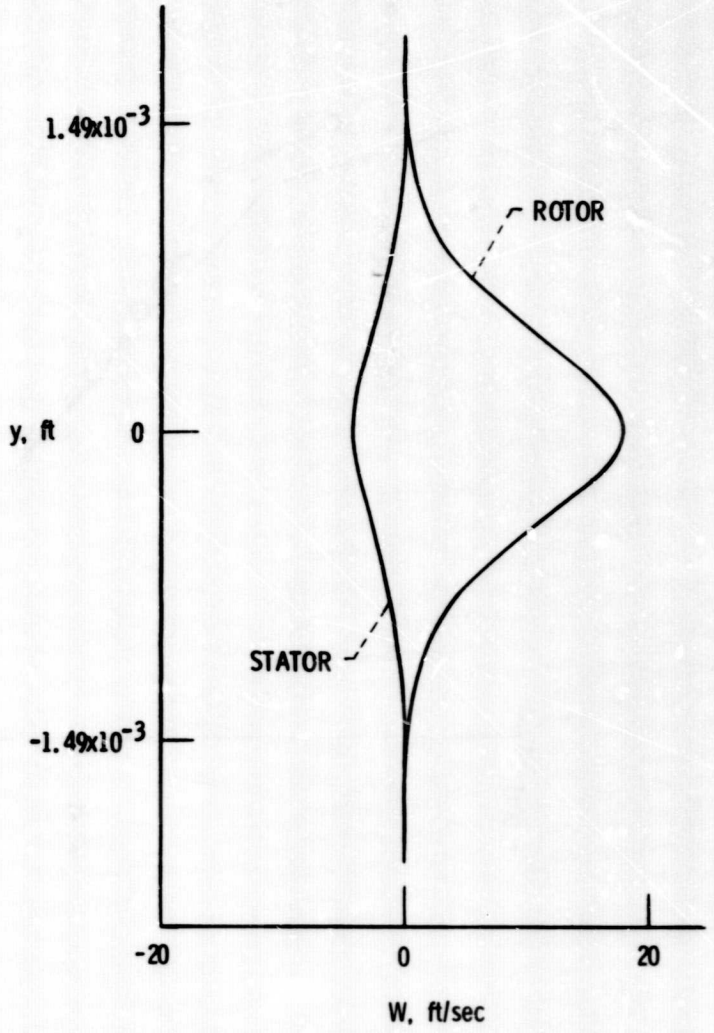

Figure 10. - Radial velocity, wake, for rotor (Ω = 200 rad/sec) and stator (Ω = 0) cases.

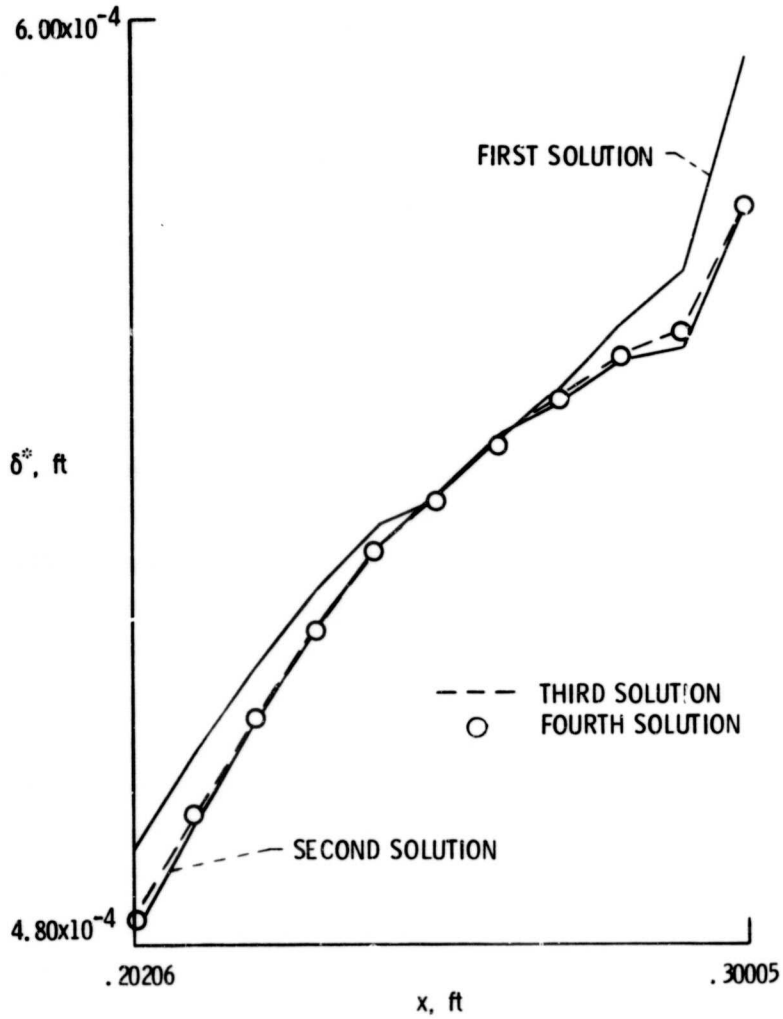

Figure 11. - Displacement thickness distributions over a rearwards portion of the suction surface.

References

1. Wu, C. H., A General Theory of Three Dimensional Flow in Subsonic Turbomachines of Axial, Radial and Mixed Flow Types, NACA TN 2604 (1952).
2. Katsanis, Theodore, FORTRAN Program for Calculating Transonic Velocities on a Blade-to-Blade Stream Surface of a Turbomachine, NASA TN D-5427 (1969).
3. Katsanis, Theodore and McNally, William D., FORTRAN Program for Calculating Velocities and Streamlines on the Hub-Shroud Mid-Channel Flow Surface of an Axial- or Mixed-Flow Turbomachine, I--User's Manual, NASA TN D-7343 (1973).
4. Horlock, J. H. and Wordsworth, J., The Three-Dimensional Laminar Boundary Layer on a Rotating Helical Blade, J. Fluid Mech., Vol. 23, Pt. 2, pp. 305-314 (1965).
5. Miyake, Y. and Fujita, S., A Laminar Boundary Layer on a Rotating Three-Dimensional Blade, J. Fluid Mech., Vol. 65, Pt. 3, pp. 481-498 (1974).
6. Mellor, G. H. and Wood, G. M., An Axial Compressor End Wall Boundary Layer Theory, Trans., ASME J. of Basic Eng., Vol. 93, No. 2 (1971).
7. Caretto, L. S., Curr, R. M. and Spalding, D. B., Two Numerical Methods for Three-Dimensional Boundary Layers, Computer Meth. in Appl. Mech. and Eng., 1, pp. 39-57 (1972).
8. Briley, W. Roger, Numerical Method for Predicting Three-Dimensional Steady Viscous Flow in Ducts, J. Comp. Phys., Vol. 14, No. 1 (1974).
9. Delaney, R. A. and Kavanagh, P., Transonic Flow Analysis in Axial-Flow Turbomachinery Cascades By a Time-Dependent Method of Characteristics, Technical (Final) Report, ERI-74034, Iowa State University, Ames, Iowa, May 1974.
10. Kurzrock, John W. and Novick, Allen S., Transonic Flow Around Compressor Rotor Blade Elements, Vol. 1: Analysis. Air Force Aero Propulsion Laboratory Report, AFAPL-TR-73-69, Vol. 1, Aug. 1973.
11. Gopalkrishnan, S. and Bozzola, R., A Numerical Technique for the Calculation of Transonic Flows in Turbomachinery Cascades, ASME Paper No. 71-GT-42, Gas Turbine Conference and Products Show, Houston, TX, March 1971.
12. Erdos, J., Alzner, E., Kalben, P., McNally, W. and Slutsky, S., Time Dependent Transonic Flow Solutions for Axial Turbomachinery, NASA SP-347, Part I, pp. 587-621 (1975).
13. MacCormack, R. W., Numerical Solution of the Interaction of a Shock Wave with a Laminar Boundary Layer, Lecture Notes in Physics, Vol. 8, Springer-Verlag, New York, pp. 151-163 (1971).
14. Briley, W. R. and McDonald, H., An Implicit Numerical Method for the Multidimensional Compressible Navier-Stokes Equations, United Aircraft Research Laboratories Report M911363-6, Nov. 1973.
15. Beam, R. M. and Warming, R. F., An Implicit Finite Difference Algorithm for Hyperbolic Systems in Conservation Law Form, J. Comp. Phys., Vol. 22, No. 1, pp. 87-110 (1976).
16. MacCormack, R. W., An Efficient Numerical Method for Solving the Time-Dependent Compressible Navier-Stokes Equations at High Reynolds Number. Paper presented at the ASME 97th Winter Annual Meeting, New York, December 5-10, 1976.
17. Olson, L. E. and Dvorak, F. A., Viscous/Potential Flow about Multi-Element Two-Dimensional and Infinite-Span Swept Wings: Theory and Experiment, NASA TMX-62, 513 (1975).
18. Brune, G. W., Rubbert, P. E. and Nark, T. C., A New Approach to Inviscid Flow/Boundary Layer Matching, AIAA Paper No. 74-601 (1974).
19. Lighthill, M. J., On Displacement Thickness, J. Fluid Mech., Vol. 4, Pt. 4, pp. 383-392 (1958).
20. Moretti, G., Importance of Boundary Conditions in the Numerical Treatment of Hyperbolic Equations. High Speed Computing in Fluid Dynamics, Physics of Fluids Supplement II, pp. II-13 — II-20 (1969).
21. Moretti, G., The Choice of a Time-Dependent Technique in Gas Dynamics, PIBAL Report No. 69-26, Polytechnic Institute of Brooklyn, July 1969.
22. Johnston, W. Sockol, P. and Reshotko, E., A Viscous-Inviscid Interactive Compressor Calculation. Report FTAS/TR-78-136, Dept. of Mech. and Aerospace Eng., Case Western Reserve University, March 1978.
23. Hornbeck, R. W., Numerical Marching Techniques for Fluid Flows with Heat Transfer, NASA SP-297 (1973).
24. Abbott, I. H. and Von Doenhoff, A. E., Theory of Wing Sections, Dover (1959).